PAPER

NJC

www.rsc.org/njc

Self-assembled monolayers of diamine molecules and phosphomolybdic acid on an ITO surface

Sang-Yoon Oh,[a] Young-Ja Yun,[a] Kyung-Hee Hyung†[b] and Sung-Hwan Han*[b]

[a] *Department of Chemistry, Soongsil University, 1-1, Sangdo-5 dong, Dongjak-gu, Seoul 156-743, Korea*

[b] *Department of Chemistry, Hanyang University, Haengdang-dong 17, Sungdong-ku, Seoul 133-791, Korea. E-mail: shhan@hanyang.ac.kr; Fax: +822-2299-0762; Tel: +822-2290-0934*

Received* (*in Montpellier, France*) *26th August 2003, Accepted 26th November 2003
First published as an Advance Article on the web 1st March 2004

Self-assembled monolayers of 1,12-diaminododecane were prepared on an ITO surface and characterized by cyclic voltammetry, imine formation, secondary ion mass spectroscopy, and Rutherford backscattering spectroscopy (RBS). The surface concentration of 1,12-diaminododecane was measured to be a maximum of 9×10^{-10} mol cm^{-2} using RBS. Utilizing the surface amine functional group on the self-assembled monolayers of 1,12-diaminododecane, secondary layers of phosphomolybdic acid were prepared and monitored by cyclic voltammetry. The self-assembled monolayers of 1,12-diaminododecane were stable both physically and chemically, and even survived after exposure to air for 4 months

1. Introduction

Indium-tin oxide (ITO) is a typical oxide material with good transparency and conductivity characteristics for flat-panel displays[1] and solar cells.[2] The formation of self-assembled monolayers (SAMs) on an ITO surface is one of the best ways to control the surface chemistry. However, due to the rough surface area, there are reservations as to the nature of the coordination mode of the functional groups on ITO. ITO films are prepared by RTE,[3] RF, DC sputtering,[4] electron beam evaporation,[5] and spray pyrolysis.[6] Due to preparation methods used, ITO films have a very high surface roughness. Such a rough morphology has been thought to be an obstacle to the formation of self-assembled monolayers and their in-depth understanding. Despite the extensive practical and potential uses of ITO, only a few studies have focused on the surface chemistry of ITO. Understanding the interactions of organic molecules on an ITO surface is challenging from the viewpoint of both fundamental and technological applications.

Moreover, the formation of self-assembled monolayers on gold surfaces has attracted a great deal of attention since the mid-80s.[7] A gold surface provides a well-defined uniform surface and can be easily investigated using conventional analytical methods. The formation of SAMs on a gold surface can easily provide control of surface properties such as the wetting angle,[8] adhesion,[9] lubrication,[10] corrosion,[11] as well as electrical properties.[12] The rich accumulation of information on SAMs has made it possible to derive many applications: sensors,[13] lithography,[14] surface passivation,[15] and surface property control.[16]

Nevertheless, the formation of self-assembled monolayers on other surfaces, in particular oxide surfaces, is poorly understood. There are few reports on the adsorption of organic or organometallic compounds on an ITO surface.[17] The chlorosilane derivatives reacted with the hydroxyl groups on the glass surface to form self-assembled monolayers attached by a silanol group.[18] The use of alkyl silanol is one of the major methodologies to prepare self-assembled monolayers on oxide surfaces. However, it is rather difficult to form dense monolayers with a good reproducibility. Carboxylic acids and phosphoric acids have also been used as adsorbents as an alternative approach to prepare self-assembled monolayers on oxide surfaces, but the adsorption can be weak.[19]

A few years ago we reported in a short communication the formation of densely packed self-assembled monolayers on an ITO surface with diamine-functionalized alkane molecules (1,12-diaminododecane).[20] The formation of self-assembled monolayers of 1,12-diaminododecane on an ITO surface effectively controlled the surface properties and allowed the preparation of secondary layers of organic or inorganic compounds on it by a reaction with its surface amine functionality. The self-assembled monolayers of 1,12-diaminododecane on ITO were further used to prepare fullerene-multilayered architectures, which showed exceptional electrochemical behavior, acting as ion selective electrodes,[21] rectifiers,[22] and electron acceptors.[23]

The surface modification of ITO is a first step for designing surface architectures. The formation of multilayer architectures on an ITO surface is one of the key issues for the development of light-induced molecular electronics. For a comprehensive understanding of self-assembled monolayers on an ITO surface, we report here systematic investigations on the structure and properties of self-assembled 1,12-diaminododecane monolayers on an ITO surface.

2. Results and discussion

2.1 Rutherford backscattering spectroscopy of self-assembled monolayers of 1,12-diaminododecane on an ITO surface

The concentration of 1,12-diaminododecane on the ITO surface was measured by Rutherford backscattering spectroscopy (RBS). RBS is a sensitive method for analyzing heavy nuclei. Light elements such as C, N, and O show weak signals. However, C gives a higher response than N and O due to the 12 carbons in 1,12-diaminododecane. As shown in Fig. 1, indium and tin showed strong signals due to their high surface

† Supported by the Brain Korea 21 Project in 2003

DOI: 10.1039/b310308k

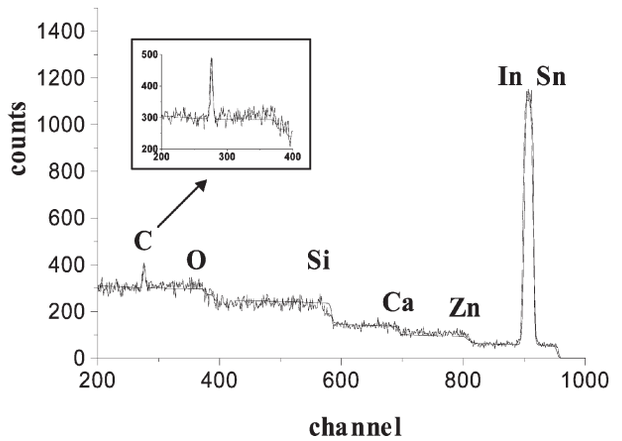

Fig. 1 Rutherford backscattering spectrum of the self-assembled monolayers of 1,12-diaminododecane on the ITO surface. The inset is a magnified carbon peak from 1,12-diaminododecane/ITO.

concentrations, while silicone and calcium signals appeared as minor impurities on the ITO surface.

For this study we performed a series of cleaning experiments and measured the residual carbon content on the ITO surface by RBS: a piranha solution (10 s), methanol sonication (2 min, two times), acetone–methanol sonication (15 min each), methanol washing. The carbon concentrations on the ITO surface after the cleaning procedures ranged from 0.65×10^{16} atom cm^{-2} to 0.83×10^{16} atom cm^{-2}. Among the several cleaning processes used, the methanol sonication method gave the lowest carbon content on the ITO surface. The cleaned ITO sample was immersed in a methanol solution with out 1,12-diaminododecane for 2 days, after which the RBS experiment was performed. The carbon atom concentration remained the same (0.65×10^{16} atom cm^{-2}), thus ruling out the possibility of carbon contamination during the immersion step.

The number of carbon atoms on the SAMs/ITO after the formation of the self-assembled monolayers of 1,12-diaminododecane was 1.3×10^{16} atoms cm^{-2}. In order to obtain the actual number of carbon atoms from 1,12-diaminododecane on the ITO surface, the number of background carbon atoms of the bare ITO needs to be subtracted because there is surface contamination even after the ITO cleaning process. The background number of carbon atoms was 0.65×10^{16} atoms cm^{-2}, which was attributed to advantageous carbon embedded in the bulk of ITO during the sputtering process of the ITO plate. The surface concentration of 1,12-diaminododecane was calculated to be 9×10^{-10} mol cm^{-2} using the following equation:

$$(1.3 \times 10^{16} - 0.65 \times 10^{16})/[12(\text{dodecane}) \times 6.02 \times 10^{23} \times (\text{Avogadro's constant})] = 9 \times 10^{-10} \text{ mol cm}^{-2}$$

This is one of the highest numbers ever reported. The quantitative measurement of the surface concentration of 1,12-diaminododecane by RBS demonstrates that this technique is a new and convenient analytical method for characterizing self-assembled monolayers.[24]

2.2. Utilization of the amine functional group generated by the formation of SAMs of 1,12-diaminododecane/ITO

The surface amine functional group is a base as well as a nucleophile. With aldehyde, the amine functional group forms an imine group when in a dry ethanol solution at 50 °C under an Ar atmosphere for 3 h.[20] The diaminododecane does not adsorb on a glass surface, as monitored by the adsorption of copper phthalocyaninetetrasulfonic acid on SAMs of diaminododecane. Also, we have performed control experiments with a blank ITO surface (no diaminododecane SAM). We could not observe any adsorption of *p*-nitrobenzaldehyde on the ITO surface within the detection limits of UV spectroscopy. The amine functional group has the same nucleophilicity as a free amine. The formation of imine was used to determine the amine concentration on ITO by hydrolysis and UV measurement of the released *p*-nitrobenzaldehyde. The 1,12-diaminododecane concentration adsorbed on the ITO surface was measured to be 6×10^{-10} mol cm^{-2}. Compared to the 9×10^{-10} mol cm^{-2} value obtained from the RBS experiment, the value of 6×10^{-10} mol cm^{-2} is a minimum because all of the amine functional groups may not react with the aldehyde to form an imine.

The amine-functionalized surface can interact with phosphomolybdic acid (heteropolyacid, HPA, $H_3[PMo_{12}O_{40}]^{-3}$) *via* an acid-base complex to form further layers.[20] Phosphomolybdic acid is a strong Brønsted acid having multiple protons.[25] In addition to its strong acidity, phosphomolybdic acid has good redox properties in aqueous media and its electrochemical behavior has been investigated.[26] Phosphomolybdic acid ($H_3PMo_{12}O_{40}$) undergoes multiple electron transfers in solution [Fig. 2(a)]. All the electrochemical measurements showed good reproducibility within the error range of 10%. When phosphomolybdic acid was adsorbed on an ITO surface, the following three distinctive two-electron reversible reductions took place [Fig. 2(b)]:[25b]

$$[PMo_{12}{}^{VI}O_{40}]^{3-} + 2e^- \rightarrow [PMo_{10}{}^{VI}Mo_2{}^{V}O_{40}]^{5-} \quad \text{(I)}$$

$$[PMo_{10}{}^{VI}Mo_2{}^{V}O_{40}]^{5-} + 2e^- \rightarrow [PMo_8{}^{VI}Mo_4{}^{V}O_{40}]^{7-} \quad \text{(II)}$$

$$[PMo_8{}^{VI}MoMo_2{}^{V}O_{40}]^{7-} + 2e^- \rightarrow [PMo_6{}^{VI}Mo_6{}^{V}O_{40}]^{9-} \quad \text{(III)}$$

The surface concentration of phosphomolybdic acid was measured by integrating the reduction current. A CV of the bare ITO in 0.1 M HCl was obtained as a blank test, which was subtracted from the CV of the phosphomolybdic acid modified ITO electrode, and integrated the reduction peaks. The surface concentration of the phosphomolybdic acid on the ITO surface without SAMS was calculated as 2.0×10^{-11} mol cm^{-2} by integrating the current of the cyclic voltammogram (Table 1). In the presence of the self-assembled monolayers of 1,12-diaminododecane, the surface concentration of the phosphomolybdic acid increased by an order of magnitude to 2.0×10^{-10} mol cm^{-2} (Table 1). The size of the

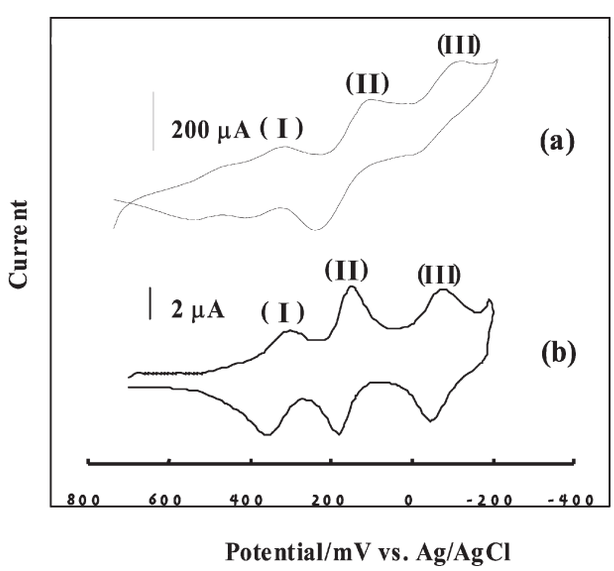

Fig. 2 Cyclic voltammograms of (a) 5×10^{-10} mol cm^{-2} phosphomolybdic acid in a 0.1 M HCl aqueous solution and (b) adsorbed phosphomolybdic acid on ITO (HPA/ITO; I, 1st 2e redox peak; II, 2nd 2e redox peak; III, 3rd 2e redox peak). Scan rate 0.2 V s^{-1}; supporting electrolyte 0.1 M HCl.

Table 1 Characteristics of the cyclic voltammograms (200 mV S^{-1} scan rate) of phosphomolybdic acid on ITO

	HPA/ITO			HPA/DD/ITO		
	Peak I	Peak II	Peak III	Peak I	Peak II	Peak III
$E_{1/2}$/mV	330	165	−63	321	157	−95
ΔE/mV	51	30	28	87	52	51
Coverage/ mol cm^{-2}	2×10^{-11}			2×10^{-10}		

spherical phosphomolybdic acid of the Keggin structure is approximately 10–12 Å.[27] The theoretical concentration of a monolayer coverage of phosphomolybdic acid on a flat surface is 1.7×10^{-10} mol cm^{-2}.[28] The roughness factor of the ITO plate was measured by reported methods in two different electrolytes in order to estimate the surface coverage.[29] The roughness factor of the ITO surface was close to 1 (0.95 in 0.1 M K_2SO_4 and 0.91 in 0.1 M $HClO_4$ solution). The conductivity of ITO originates from the formation of reduced indium sites in ITO. The conductivity of ITO is controlled by changing the atmospheric conditions during the ITO sputtering process. Also, the SIMS data in Fig. 5 (below) showed the amine adsorption to be at the metallic indium site. Considering the physical roughness of the ITO surface, a roughness close to 1 suggests that all the surface is not providing adsorption sites, and the total area for the amine adsorption is close to the apparent ITO area. Considering the surface roughness, the surface concentration of 2.0×10^{-10} mol cm^{-2} indicates complete monolayer coverage of phosphomolybdic acid on the 1,12-diaminododecane self-assembled monolayers.

The surface concentration of the amine was 6.0×10^{-10} mol cm^{-2} from the imine formation experiment as a minimum value and 9.0×10^{-10} mol cm^{-2} from the RBS experiment as a maximum value. The phosphomolybdic acid concentration measured by cyclic voltammetry was 2.0×10^{-10} mol cm^{-2}. The theoretical surface concentration of 1,12-diaminododecane should be three times higher than that of phosphomolybdic acid with three protons. However, not all the 1,12-diaminododecane will form an acid-base complex with phosphomolybdic acid due to the ITO surface morphology, and the ratio of 1,12-diaminododecane and the heteropolyacid should be 3 or more than 3. The experimental ratio is a minimum 3:1 to a maximum of 4.5:1, which coincides with the stoichiometric considerations.

Phosphomolybdic acid adsorption on the self-assembled monolayer of 1,12-diaminododecane was confirmed by changing the scan rate of the cyclic voltammetry. If the electroactive molecules are dissolved in solution, the peak currents of the cyclic voltammogram will be linear with the square root of the scan rate ($\nu^{1/2}$).[30] A plot of the peak current of the first redox wave showed good linearity with the scan rate, which means that phosphomolybdic acid was adsorbed on the electrode surface (Fig. 3).[30] The self-assembled monolayer of 1,12-diaminododecane and the second layer of phosphomolybdic acid are stable even under such strong acidic conditions (0.1 M HCl solution) and survived repeated cyclic voltammetry scans.

2.3. Electrochemical characterization of self-assembled monolayers of 1,12-diaminododecane with phosphomolybdic acid layers

Electron transfer between the ITO surface and phosphomolybdic acid was monitored by cyclic voltammetry. Without the self-assembled monolayers of 1,12-diaminododecane, there would be no electron transfer barrier. Fig. 4(a) shows there was little change in the peak potential separation of the reduction and oxidation waves on the ITO surface. The differences in the peak-to-peak separation ($\Delta E = E_{anode} - E_{cathode}$) were 50, 30, and 30 mV on the ITO surface, which increased to 90, 50, and 50 mV in the presence of the self-assembled monolayers of 1,12-diaminododecane on the surface (Table 1). As the scan rate was increased, the peak-to-peak separation also increased, indicating the occurrence of charge transfer retardation as a result of the long alkyl chains (Table 2). The electron transfer retardation took place for all of the three two-electron transfer processes. In the first two-electron transfer waves, ΔE increased from 50 to 60 mV as the scan rate was increased from 200 to 1000 mV s^{-1} on the bare ITO. In contrast, in the presence of the self-assembled 1,12-diaminododecane monolayers, electron transfer retardation increased from 90 to 130 mV as the scan rate was increased from 200 to 1000 mV s^{-1}. At 1000 mV s^{-1}, the difference of $\Delta E(I)^b - \Delta E(I)^a$/ mV doubled that obtained at 200 mV s^{-1}.

Another characteristic of the phosphomolybdic acid layers on the 1,12-diaminododecane self-assembled monolayers is the negative shift in the formal potentials [$E_{1/2} = (E_{cathode} + E_{anode}/2)$]. The formal potentials of phosphomolybdic acid on the self-assembled monolayers shifted in the negative direction by 10, 10, and 30 mV, respectively (Table 1). The negative shift can be attributed to the formation of an electrostatic charge complex of the anionic $PMo_{12}O_{40}^{-3}$ compound with the surface amine functional groups.

2.4. Identification of amine adsorption sites on the ITO surface by SIMS

Structural information about the surface was collected by secondary ion mass spectroscopy (SIMS). The ITO surface, which was prepared using a sputtering method, consists of indium

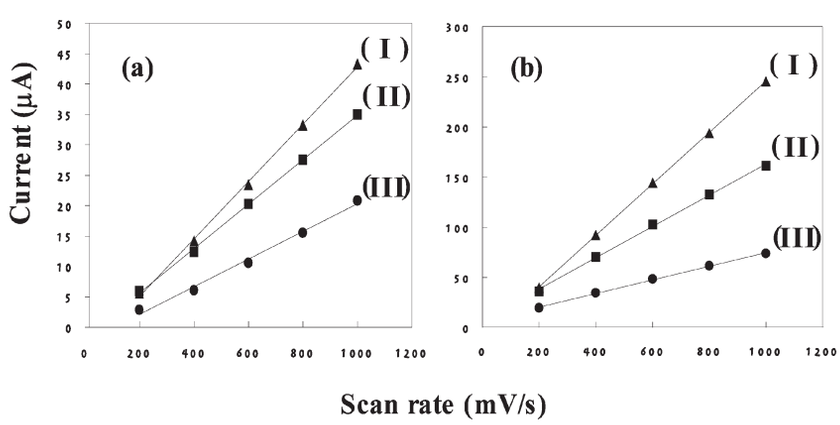

Fig. 3 Plots of the peak current *versus* the scan rate from the cyclic voltammograms of (a) phosphomolybdic acid/ITO and (b) phosphomolybdic acid/1,12-diaminododecane/ITO in Fig. 4 (I, 1st redox peak; II, 2nd redox peak; III, 3rd redox peak).

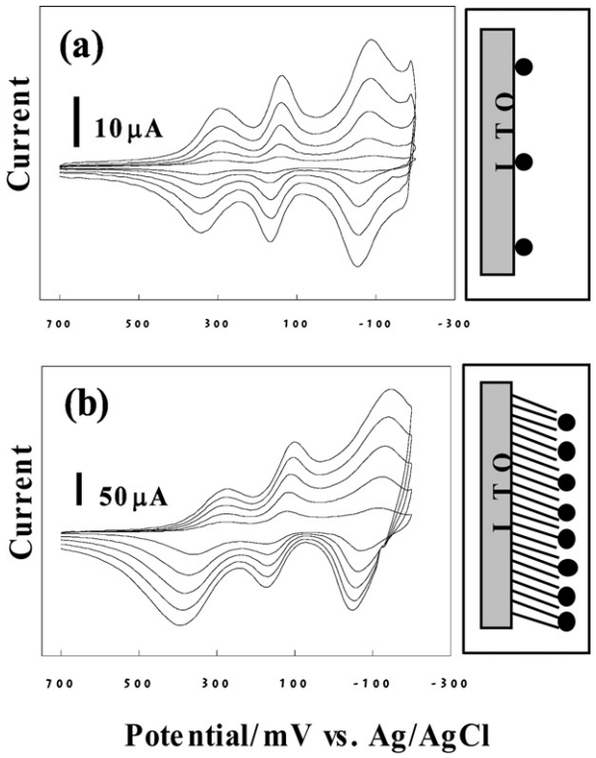

Fig. 4 Cyclic voltammograms of phosphomolybdic acid adsorbed on (a) bare ITO and (b) 1,12-diaminododecane/ITO in 0.1 M HCl/H_2O at different scan rates (200, 400, 600, 800, 1000 mV s^{-1}). The diagrams on the right side of the cyclic voltammograms represent the idealized surface structures of phosphomolybdic acid/ITO and phosphomolybdic acid/1,12-diaminododecane/ITO.

oxide and tin oxide in a 9:1 ratio. Due to the heterogeneity of the ITO surface, several coordination modes of 1,12-diaminododecane on the ITO surface are possible. These are coordination to indium metal, indium oxide, tin metal, and tin oxide. Mass fragments containing indium and tin were collected and analyzed by the SIMS experiments. A comparison of the mass intensities of the bare ITO and the 1,12-diaminododecane/ITO made it possible to understand the surface coordination sites. As shown in Fig. 5(a,b), the carbon, nitrogen and oxygen peaks from 1,12-diaminododecane on ITO were compared with those of the bare ITO. The signal intensities from the surface oxygen and hydroxyl groups are almost similar for both surfaces. The chlorine signals also did not alter after the formation of the self-assembled 1,12-diaminododecane monolayers. The oxygen signal intensity were used as the standard value for calculating the intensity ratio between the bare ITO and the 1,12-diaminododecane/ITO. Due to the high signal-to-noise ratio of SIMS, the background showed intrinsic impurities of carbon and nitrogen too.

In the presence of the 1,12-diaminododecane SAMs, the molecular peaks from CN and CNO increased in concentration,

Table 2 Peak-to-peak separation in Fig. 4 of the 1st redox peak *versus* the scan rate

		Scan rate/mV s^{-1}				
	System	200	400	600	800	1000
ΔE(I)/mV	HPA/ITO[a]	51	59	57	60	62
	HPA/DD/ITO[b]	87	97	109	120	126
$\Delta E(I)^b - \Delta E(I)^a$/mV	—	36	38	52	61	64

[a] Phosphomolybdic acid/ITO. [b] Phosphomolybdic acid/1,12-diaminododecane/ITO.

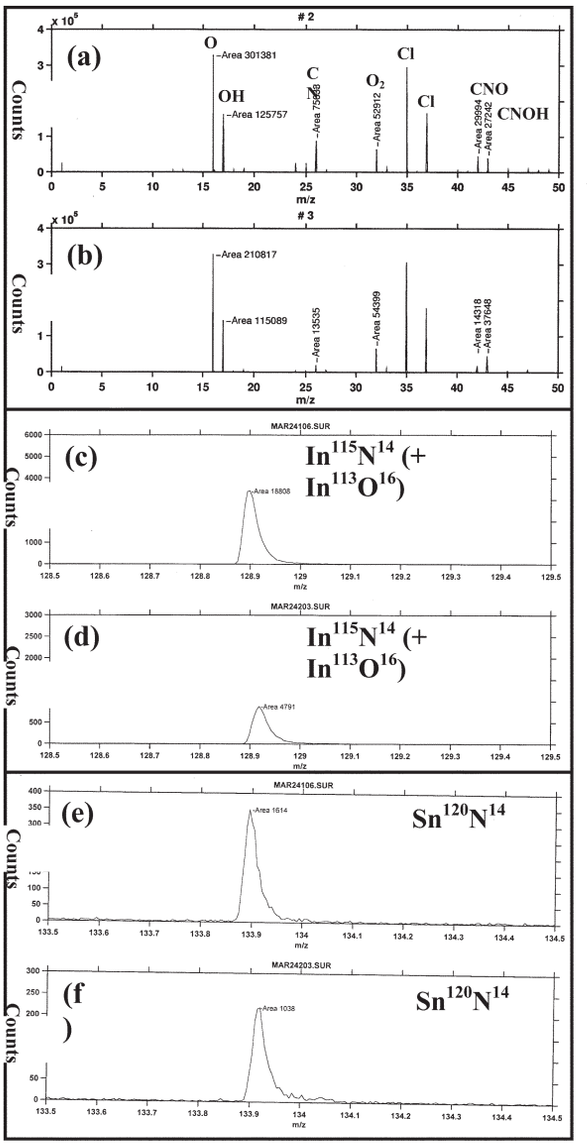

Fig. 5 Secondary ion mass spectra of (a) 1,12-diaminododecane/ITO and (b) bare ITO; $m/z = 129$ corresponding to $In^{115}N^{14}$ from (c) 1,12-diaminododecane/ITO and (d) bare ITO; $m/z = 134$ corresponding to $Sn^{120}N^{14}$ from (e) 1,12-diaminododecane/ITO and (f) bare ITO.

indicating the presence of amine functional groups on the ITO surface. The nitrogen containing peaks were divided by the area of the reference oxygen peak, yielding a ratio of 1:4.4 of the nitrogen containing peaks between the bare ITO and 1,12-diaminododecane/ITO. As we will see below, the ratio of 1:4.4 is a key reference number for deducing the surface coordination position of 1,12-diaminododecane.

The molecular peak of $m/z = 129$ was monitored as an indication of the presence of $In^{115}N^{14}$ [Fig. 5(c,d)]. There is a 95.7% natural abundance of In^{115} with the rest being In^{113}. The signal at $m/z = 129$ signals the presence of an In–N bond, indicating coordination of 1,12-diaminododecane on the metallic indium site. The signal at $m/z = 129$ from 1,12-diaminododecane/ITO increased more strongly than that from the bare ITO. The peak area integrated from the bare ITO and 1,12-diaminododecane/ITO was normalized to the areas of the oxygen reference peaks. The ratio of the signal at $m/z = 129$ for the bare ITO and 1,12-diaminododecane/ITO was 1:3.9, which was close to that of CN (1:4.4). The increase in the CN intensity indicates an increase in the 1,12-diaminododecane molecule concentration on the ITO surface while the strong signal increment at $m/z = 129$ suggests the coordination of the nitrogen of 1,12-diaminododecane to the metallic indium.

The possibility of tin coordinating with the amine was also monitored at $m/z = 134$, corresponding to $Sn^{120}N^{14}$ [Fig. 5(e,f)]. The signal areas were divided by the reference oxygen signals and the ratio between the bare ITO and 1,12-diaminododecane/ITO was 1:1.1. Basically, there was little change in the signal intensity at $m/z = 134$, essentially ruling out the coordination of 1,12-diaminododecane to metallic tin. Another possibility was the coordination of the amine to the metal oxide or metal hydroxide. The peaks at $m/z = 145$ ($In^{115}O^{16}N^{14}$) and $m/z = 150$ ($Sn^{120}O^{16}N^{14}$) were monitored and compared to each other. The signal ratios between the bare ITO and the 1,12-diaminododecane/ITO were 1:1.8 and 1:1.2 in the InON and SnON, respectively. The slight increase in the ratios indicates a minor contribution of 1,12-diaminododecane coordination to the metal oxides through hydrogen bonding, particularly in indium oxide.

2.5. Formation kinetics of the self-assembled monolayers

The easy formation of the second layers of the heteropolyacid enabled the formation kinetics of the self-assembled monolayers to be monitored by electrochemistry. After the self-assembled monolayers were formed over a certain time period at 50 °C, the ITO plate was washed completely with dry methanol and water, followed by the dipping in a 5×10^{-4} M phosphomolybdic acid–0.1 M HCl aqueous solution. The formation of the second layers of phosphomolybdic acid is a fast process due to the acid-base complex formation reaction and was completed in one minute. The concentration of 1,12-diaminododecane on the ITO surface is directly proportional to that of the phosphomolybdic acid. After soaking the ITO plate in the 1,12-diaminododecane solution, the current density of the heteropoly acid on the ITO plate was monitored by cyclic voltammetry. The surface concentrations were calculated based on an integration of the redox current (Fig. 6). The initial rate for the adsorption of 1,12-diaminododecane was quite fast and the coverage reached 56% after 5 h. The maximum surface concentration of 2.4×10^{-10} mol cm^{-2} phosphomolybdic acid was obtained in 48 h. After 48 h, the surface was almost saturated with the self-assembled monolayers.

It is known that self-assembled monolayers of alkyl thiolate on a gold surface attain as much as 70–80% of the maximum coverage within 1 h.[31] The formation of the 1,12-diaminododecane self-assembled monolayers on the ITO surface is a relatively slow process compared to that of alkyl thiolate on a gold surface. However, the pattern of self-assembled monolayer formation on ITO is similar to that on a gold surface: the fast adsorption of molecules onto the surface followed by a rearrangement in the presence of lateral interactions such as van der Waals interactions and hydrogen bonding.[32]

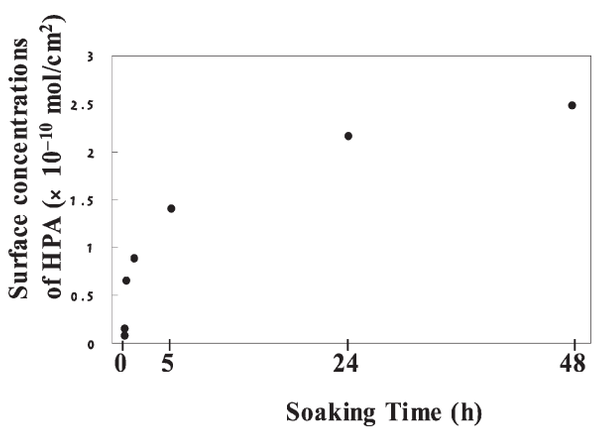

Fig. 6 Surface coverage of phosphomolybdic acid on 1,12-diaminododecane/ITO as a function of the soaking time of 1,12-diaminododecane/ITO in methanol at 50 °C (soaking times were 10 s, 1 min, 10 min, 1 h, 5 h, 24 h and 48 h in 1,12-diaminododecane–methanol solution; soaking time in 5×10^{-4} M phosphomolybdic acid–0.1 M HCl–H_2O was 1 min).

2.6. Effects of chain length on the formation of self-assembled monolayers on ITO

The formation of the secondary layers of phosphomolybdic acid enabled the effects of chain length to be investigated and the kinetic effects on the formation of self-assembled monolayers on the ITO surface to be monitored. The peak area calculated by integrating the cyclic voltammogram of phosphomolybdic acid represented the 1,12-diaminododecane concentration on ITO.

Diamine molecules with different carbon numbers [ethylenediamine (C_2), 1,6-hexamethylenediamine (C_6), 1,8-diaminooctane (C_8), 1,10-diaminodecane (C_{10}), and 1,12-diaminododecane (C_{12})] were used in this investigation. Each sample was prepared under identical conditions: 2 days in the diaminoalkane solution followed by dipping in a 5×10^{-4} M phosphomolybdic acid–0.1 M HCl aqueous solution for 5 min. As shown in Fig. 7, no self-assembled monolayers were formed when diamines having a carbon chain length of up to and including 6 were used. The current densities from the diamines with less than 8 carbons were almost identical to the base line of the bare ITO. The current density abruptly jumped when the carbon chain length was 8 (1,8-diaminooctane). The formation of self-assembled monolayers with diamines having a carbon chain length of 8 or more exhibited a similar contribution from the van der Waals interactions between the alkyl chains as observed in the case of alkyl thiols on gold.[18] The formation of SAMs with longer carbon chains also excludes the possibility of the diamine bonding in a hairpin loop mode. If hairpin loop formation is the preferred bonding mode, diamines with longer chains will have a greater tendency to form hairpin loops than those with shorter chains. The experimental results showed that the surface of the SAMs was functionalized by the amine group and reacted with acidic phosphomolybdic acid.

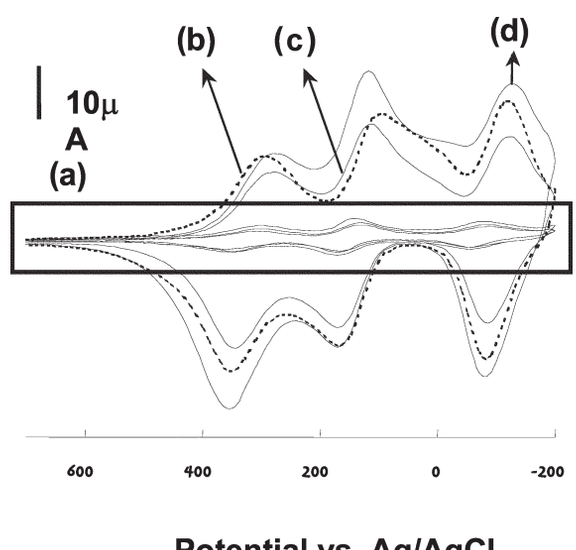

Fig. 7 Cyclic voltammograms of phosphomolybdic acid adsorbed on (a) bare ITO, ethylenediamine(C2)/ITO and hexamethylenediamine (C6)/ITO, (b) 1,8-diaminooctane(C8)/ITO, (c) 1,10-diaminodecane(C10)/ITO and (d)1,12-diaminododecane(C12)/ITO. Scan rate, 0.2 V s^{-1}; supporting electrolyte, 0.1 M HCl.

2.7. Stability of 1,12-diaminododecane self-assembled monolayers on ITO surface

One of the drawbacks for the practical application of alkyl thiols on a gold surface is the poor stability of the sulfur functional group, which is easily oxidized on the gold surface. Sulfur compounds are susceptible to oxidation to sulfur oxide, particularly on a metallic surface. The advantage of the nitrogen functional groups is its chemical stability towards oxidation and reduction.

The self-assembled monolayers of 1,12-diaminododecane on ITO were extremely stable under the strongly acid conditions of a 0.1 M HCl solution in water for 20 h. The results indicate that the amine functional group of 1,12-diaminododecane has a good affinity for the ITO surface. Moreover, it even survived under sonication in water for 2 min and was not damaged by exposure to air for 4 months. After 4 months exposure to air, the self-assembled monolayers of 1,12-diaminododecane on the ITO surface were dipped in a phosphomolybdic acid solution, which recovered its original current density. Such excellent physical and chemical stability is attributed to the combination of van der Waals interactions of the alkyl chains, amine adsorption on indium, and interactions between the terminal amine functional groups.

The formation of self-assembled monolayers of 1,12-diaminododecane on ITO is a slow process, while the adsorption of phosphomolybdic acid on 1,12-diaminododecane/ITO is fast (<1 min). Phosphomolybdic acid adsorbed on 1,12-diaminododecane/ITO was slowly released in a 0.1 M HCl solution and the current density decreased by 40% after 3 h. The adsorption and desorption of the heteropolyacid on the self-assembled monolayers is a reversible process and the reduced current density is easily recovered by immersing the 1,12-diaminododecane/ITO plate into a phosphomolybdic acid solution.

3. Conclusions

This study demonstrated the formation of stable self-assembled monolayers of 1,12-diaminododecane on an ITO surface, as well as the formation of secondary layers of phosphomolybdic acid and amine groups on 1,12-diaminododecane/ITO. Quantitative measurements of the surface concentration of 1,12-diaminododecane by RBS and the imine formation reaction gave a minimum of 6×10^{-10} mol cm^{-2} and a maximum of 9×10^{-10} mol cm^{-2}. Further, the diamine concentration on the ITO surface was easily monitored by electrochemistry of the second layers of phosphomolybdic acid as a probe molecule, which can be adsorbed on three amine functional groups. The quick and easy characterization of the 1,12-diaminododecane/ITO system by the electrochemistry of phosphomolybdic acid enabled the monitoring of the electron transfer retardation through the alkyl chains of 1,12-diaminododecane, the formation kinetics, and its stability to be examined.

The formation of self-assembled monolayers on the ITO surface and their characterization have long been a challenging target from the viewpoint of both fundamental and technological applications. The results presented in this report are from a comprehensive study on the modification of an ITO surface with self-assembled monolayers. The modification of the ITO surface with amine functional groups is a key step to building molecular architectures on the ITO surface. The formation of stable and dense self-assembled monolayers on the ITO surface may open new opportunities for the modification and utilization of ITO surfaces. Further studies in this direction are currently under way.

4. Experimental

4.1 Materials and reagents

Solvents such as methanol and ethanol were used as purchased (J. T. Baker; HPLC grade). High purity water (Milli-Q, Millipore) was used for all experiments. For the fabrication of the monolayers on an ITO surface, ethylenediamine ($H_2NCH_2CH_2NH_2$, Aldrich; 99%), hexamethylenediamine [$H_2N(CH_2)_6NH_2$, Aldrich; 98%], 1,8-diaminooctane [$H_2N(CH_2)_8NH_2$, Aldrich; 98%], 1,10-diaminodecane [$H_2N(CH_2)_{10}NH_2$, Aldrich;97%], 1,12-diaminododecane [$H_2N(CH_2)_{12}NH_2$, Aldrich; 98%],*p*-nitrobenzaldehyde (Janssen Chimica; 99%), phosphomolybdic acid hydrate ($H_3PMo_{12}O_{40}{\cdot}xH_2O$, Aldrich; A.C.S. reagent) were also used as received. The indium-tin oxide (ITO) coated glass slides were purchased from Samsung Corning Co. and HOYA Co.

4.2 Instrumentation

The electrochemical measurements were performed using a M273A potentiostat (EG&G, PAR). A single compartment with a standard three-electrode glass cell was used with Ag/AgCl as a reference electrode (internal solution: saturated KCl aqueous solution) and Pt wire as the counter electrode. The area of the ITO electrode exposed to the solution was maintained at a constant 1 cm^2. The aqueous phase measurements were conducted under nitrogen-deaerated conditions. In order to calculate the surface concentration of phosphomolybdic acid, cyclic voltammetry was performed using bare ITO in a 0.1 M HCl solution to obtain a baseline as a blank test. Subsequently, the CV of phosphomolybdic acid on the ITO surface was aligned on the base line, and the concentration of phosphomolybdic acid on ITO was obtained from integration of the second reduction peak.

The spectroscopic measurements were carried out using Rutherford backscattering spectroscopy (RBS, which was performed at the KIST–RBS facility with a 2 MeV He^{2+} ion source), time-of-flight secondary ion mass spectroscopy (TOF-SIMS; Perkin–Elmer; 8.0 keV Cs^+ ions were used for all data reported in this paper) and UV spectroscopy (Varian, CARY100 spectrophotometer).

4.3 Sample preparation and characterization

The ITO plates were cut into 0.5×5 cm^2 pieces and cleaned in a sonication bath with acetone (15 min), followed by washing with deionized water (15 min) and finally with absolute methanol (15 min). The electrodes were stored in an absolute methanol solution in a sealed container and dried in vacuum of 10^{-3} Torr prior to use. All the electrochemical measurements showed good reproducibility with an error range of 10%. The surface roughness was measured using the reported method.[24]

The self-assembled monolayers were prepared by immersing the ITO electrodes in 5 mM solution of 1,12-diaminododecane in methanol at 20–50 °C under an Ar atmosphere for 48 h. The self-assembled monolayers on the ITO surface were then rinsed sequentially with copious amounts of methanol and water and dried under vacuum. The self-assembled monolayers of 1,12-diaminododecane on the ITO surface were investigated using RBS and TOF-SIMS. Secondary layers of phosphomolybdic acid were fabricated by dipping the SAMs/ITO electrodes in 5×10^{-4} M phosphomolybdic acid in a 0.1 M HCl aqueous solution for 5 min. The electrodes were then thoroughly washed with a 0.1 M HCl aqueous solution with magnetic stirring and dried under vacuum. The phosphomolybdic acid/1,12-diaminododecane/ITO electrodes were examined using cyclic voltammetry and AFM.[20] The surface amine functional group reacted with *p*-nitrobenzaldehyde to form secondary imine layers.[20,25] 1,12-Diaminododecane/ITO was dipped into an anhydrous ethanol solution of *p*-nitrobenzaldehyde at 50 °C under an Ar atmosphere for 3 h. The substrate was then washed and cleaned ultrasonically with absolute ethanol and dried under vacuum. The imine compound thus formed was

hydrolyzed at 30 °C for 1 h in water, and the hydrolyzed *p*-nitrobenzaldehyde was quantified using UV spectroscopy.

Acknowledgements

This work was supported by the National R&D Project for Nano-Science and Technology, Korea.

References

1 (*a*) K. L. Purvis, G. Lu, J. Schwartz and S. L. Bernasek, *J. Am. Chem. Soc.*, 2000, **122**, 1808–1809; (*b*) B. H. Lee, I. G. Kim, S. W. Cho and S. H. Lee, *Thin Solid Films*, 1997, **302**, 25–30; (*c*) J. Staudigel, M. Stößel, F. Steuber, J. Blässing and J. Simmerer, *Synth. Met.*, 2000, **111–112**, 69–73.

2 (*a*) H. Imahori, T. Azuma, A. Ajavakom, H. Norieda, H. Yamada and Y. Sakata, *J. Phys. Chem. B*, 1999, **103**, 7233–7237; (*b*) D. König and G. Ebest, *Sol. Energy Mater. Sol. Cells*, 1998, **56**, 67–74.

3 (*a*) W. J. Spence, *J. Appl. Phys.*, 1967, **38**, 3767–3770; (*b*) A. Amaral, P. Brogueira, C. Nunes de Carvalho and G. Lavareda, *Surf. Coat. Technol.*, 2000, **125**, 151–156.

4 (*a*) R. Tueta and M. Braguier, *Thin Solid Films*, 1981, **80**, 143–148; (*b*) L. J. Meng, A. Maçarico and R. Martins, *Vacuum*, 1995, **46**, 673–680.

5 R. Banerjee, D. Das, S. Ray and A. Batabyal, *Sol. Energy Mater.*, 1985, **13**, 11.

6 H. Bisht, H. T. Eun, A. Mehrtens and M. A. Aegerter, *Thin Solid Films*, 1999, **351**, 109–114.

7 (*a*) A. Ulman, *An Introduction to Ultra-thin Organic Films*, Academic Press, Boston, 1991; (*b*) L. H. Dubois and R. G. Nuzzo, *Annu. Rev. Phys. Chem.*, 1992, **43**, 437; (*c*) C. D. Bain and G. M. Whitesides, *Angew. Chem., Int. Ed. Engl.*, 1989, **28**, 506–512; (*d*) W. B. Caldwell, D. J. Campbell, K. Chen, B. R. Herr, C. A. Mirkin, A. Malik, M. K. Durbin, P. Dutta and K. G. Huang, *J. Am. Chem. Soc.*, 1995, **117**, 6071–6082; (*e*) M. D. Porter, T. B. Bright, D. L. Allara and C. E. D. Chidsey, *J. Am. Chem. Soc.*, 1987, **109**, 3559–3568; (*f*) C. D. Bain, F. B. Troughton, Y. T. Tao, J. Evall, G. M. Whitesides and R. G. Nuzzo, *J. Am. Chem. Soc.*, 1989, **111**, 321–335.

8 (*a*) J. T. Woodward, H. Gwin and D. K. Schwartz, *Langmuir*, 2000, **16**, 2957–2961; (*b*) Y. F. Miura, M. Takenaga, T. Koini, M. Graupe, N. Garg, R. L. Graham and T. R. Lee, *Langmuir*, 1998, **14**, 5821–5825.

9 R. A. Quon, A. Ulman and T. K. Vanderlick, *Langmuir*, 2000, **16**, 3797–3802.

10 H. Zarrad, J. M. Chovelon, P. Clechet, N. Jaffrezic-Renault, C. Martelet, M. Belin, H. Perez and Y. Chevalier, *Sens.Actuators, A*, 1995, **46–47**, 598–600.

11 (*a*) P. E. Laibinis and G. M. Whitesides, *J. Am. Chem. Soc.*, 1992, **114**, 9022; (*b*) G. K. Jennings, J. C. Munro, T. H. Yong and P. E. Laibinis, *Langmuir*, 1998, **14**, 6130.

12 D. Acevedo and H. D. Abruna, *J. Phys. Chem.*, 1991, **95**, 9590–9594.

13 (*a*) S. Steinberg, Y. Tor, E. Sabatania and I. Rubinstein, *J. Am. Chem. Soc.*, 1991, **113**, 5176–5182; (*b*) O. Chailapakul and R. M. Crooks, *Langmuir*, 1995, **11**, 1329–1340; (*c*) K. Bandyopadhyay, L. Shu, H. Liu and L. Echegoyen, *Langmuir*, 2000, **16**, 2706–2714.

14 (*a*) N. L. Jeon, R. G. Nuzzo, Y. Xia, M. Mrksich and G. M. Whitesides, *Langmuir*, 1995, **11**, 3024–3026; (*b*) S. Walheim, R. Müller, M. Sprenger, E. Loser, J. Mlynek and U. Steiner, *Adv. Mater.*, 1999, **11**, 1431–1433; (*c*) J. Aizenberg, A. J. Black and G. M. Whitesides, *Nature (London)*, 1999, **398**, 495–498.

15 F. P. Zamborini and R. M. Crooks, *Langmuir*, 1998, **14**, 3279–3286.

16 K. Hu and A. J. Bard, *Langmuir*, 1997, **13**, 5114–5119.

17 (*a*) T. Kondo, M. Takechi, Y. Sato and K. Uosaki, *J. Electroanl. Chem.*, 1995, **381**, 203–209; (*b*) T. J. Gardner, C. D. Frisibie and M. S. Wrighton, *J. Am. Chem. Soc.*, 1995, **117**, 6927–6933; (*c*) T. J. Meyer, G. J. Meyer, B. W. Pfenning, J. R. Schoonover, C. J. Timpson, J. F. Wall, C. Kobusch, X. Chen, B. M. Peek, C. G. Wall, W. Ou, B. W. Erickson and C. A. Bignozzi, *Inorg. Chem.*, 1994, **33**, 3952–3964; (*d*) G. Zotti, S. Zecchin, G. Schiavon, A. Berlin, G. Pagani and A. Canavesi, *Langmuir*, 1997, **13**, 2694–2698; (*e*) G. Zotti, G. Schiavon, S. Zecchin, A. Berlin and G. Pagani, *Langmuir*, 1998, **14**, 1728–1733; (*f*) Y. Obeng and A. J. Bard, *Langmuir*, 1991, **7**, 195–201; (*g*) M. E. Napier and H. Thorp, *Langmuir*, 1997, **13**, 6342–6344; (*h*) A. Berlin, G. Zotti, G. Schiavon and S. Zecchin, *J. Am. Chem. Soc.*, 1998, **120**, 13 453–13 460; (*i*) M. S. Pyon, R. J. Cherry, A. J. Bjornsen and D. C. Zapien, *Langmuir*, 1999, **15**, 7040–7046; (*j*) A. Fang, H. T. Ng, X. Su and S. F. Y. Li, *Langmuir*, 2000, **16**, 5221–5226; (*k*) S. F. J. Appleyard, S. R. Day, R. Pickford and M. R. Willis, *J. Mater. Chem.*, 2000, **10**, 169–173; (*l*) C. K. Luscombe, H. W. Li, W. T. S. Huck and A. B. Holmes, *Langmuir*, 2003, **19**, 5273–5278.

18 (*a*) A. Ulman, *Chem. Rev.*, 1996, **96**, 1533–1554; (*b*) P. Silberzan, L. Léger, D. Ausserré and J. J. Benattar, *Langmuir*, 1991, **7**, 1647.

19 (*a*) C. Yan, M. Zharnikov, A. Gölzhäuser and M. Grunze, *Langmuir*, 2000, **16**, 6208–6215; (*b*) D. L. Allara, S. V. Atre, C. A. Ellinger and R. G. Snyder, *J. Am. Chem. Soc.*, 1991, **113**, 1852–1854; (*c*) E. L. Smith and M. D. Porter, *J. Phys. Chem.*, 1993, **97**, 8032–8038; (*d*) Y. T. Tao, *J. Am. Chem. Soc.*, 1993, **115**, 4350–4358; (*e*) J. P. Folkers, C. B. Gorman, P. E. Laibinis, S. Buchholz and G. M. Whitesides, *Langmuir*, 1995, **11**, 813–824.

20 S. Y. Oh, Y. K. Yun, D. Y. Kim and S. H. Han, *Langmuir*, 1999, **15**, 4690–4692.

21 S. Y. Oh and S. H. Han, *Langmuir*, 2000, **16**, 6777–6779.

22 S. Y. Oh and S. H. Han, *Synth. Met.*, 2001, **121**, 1369–1370.

23 K. H. Hyung and S. H. Han, *Synth. Met.*, 2003, **137**, 1441–1442.

24 (*a*) G. Jarzabek and Z. Borkowska, *Electrochim. Acta*, 1997, **42**, 2915; (*b*) R. Woods, in *Chemisorption at Electrodes*, ed. A. J. Bard, Marcel Dekker Inc., New York, 1976, vol. 9, p 125.

25 (*a*) N. Mizuno and M. Misono, *Chem. Rev.*, 1998, **98**, 199–217; (*b*) M. Sadakane and E. Steckhan, *Chem. Rev.*, 1998, **98**, 219–237; (*c*) D. E. Katsoulis, *Chem. Rev.*, 1998, **98**, 359–387.

26 (*a*) A. Kuhn and F. C. Anson, *Langmuir*, 1996, **12**, 5481–5488; (*b*) C. Sun, J. Zhao, H. Xu, Y. Sun, X. Zhang and J. Shen, *J. Electroanal. Chem.*, 1997, **435**, 63–68; (*c*) C. Rong and F. C. Anson, *Inorg. Chim. Acta*, 1996, **242**, 11–16; (*d*) B. Keita, A. Belhouari and L. Nadjo, *J. Electroanal. Chem.*, 1993, **355**, 235–251; (*e*) D. Ingersoll, P. J. Kulesza and L. R. Faulkner, *J. Electrochem. Soc.*, 1994, **141**, 140–147; (*f*) S. Liu, Z. Tang, Z. Shi, Li Niu, E. Wang and S. Dong, *Langmuir*, 1999, **15**, 7268–7275; (*g*) L. Cheng, L. Niu, J. Gong and S. Dong, *Chem. Mater.*, 1999, **11**, 1465–1475.

27 I. K. Song, M. S. Kaba and M. A. Barteau, *J. Phys. Chem.*, 1996, **100**, 17 528–17 534.

28 B. Wang and S. Dong, *Electrochim. Acta*, 1996, **41**, 895.

29 J. H. Moon, J. H. Kim, K. J. Kim, T. H. Kang, B. S. Kim, C. H. Kim, J. H. Hahn and J. W. Park, *Langmuir*, 1997, **13**, 4305–4310.

30 A. J. Bard and L. R. Faulkner, *Electrochemical Methods*, John Wiley & Sons, New York, 1980, pp. 519–531.

31 F. Bensebaa, R. Voicu, L. Huron, T. H. Ellis and E. Kruus, *Langmuir*, 1997, **13**, 5335–5340.

32 (*a*) J. B. Schlenoff, M. Li and H. Ly, *J. Am. Chem. Soc.*, 1995, **117**, 12 528–12 536; (*b*) E. Cooper and G. J. Leggett, *Langmuir*, 1999, **15**, 1024–1032.